Supporting Information for

A novel 1D dysprosium chain with slow magnetic relaxation constructed by a pyridine-N-oxide ligand

Qi Chen[a], Yin-Shan Meng[b], Yi-Quan Zhang [c], Shang-Da Jiang,[d] Hao-Ling Sun[a]* and Song Gao[b]*

[a] *Department of Chemistry and Beijing Key Laboratory of Energy Conversion and Storage Materials, Beijing Normal University, Beijing 100875, P. R. China. E-mail: haolingsun@bnu.edu.cn;*

[b] *Beijing National Laboratory for Molecular Sciences, State Key Laboratory of Rare Earth Materials Chemistry and Applications, College of Chemistry and Molecular Engineering, Peking University, Beijing 100871, China. E-mail: gaosong@pku.edu.cn;*

[c] *Jiangsu Key Laboratory for NSLSCS, School of Physical Science and Technology, Nanjing Normal University, Nanjing 210023, P. R. China.*

[d] *1. Physikalisches Institut, Universität Stuttgart, Pfaffenwaldring 57, D-70550, Stuttgart, Germany.*

Experimental Section

All the starting materials were commercially available reagents for analytical grade and used without further purification.

Syntheses of HL: The Schiff-base HL ligand is synthesized by condensation of pyridine-N-oxide-2-carbohydrazide and salicyladehyde in 1:5 ratios in methanol, and then re-crystallize in 1,2-dichloroe-ethane solvent.

$[Dy(L)\cdot 4H_2O]\cdot 2Cl\cdot 2H_2O$ (1): HL (0.2mmol, 0.0572g) was dissolved in a mixed solvent of methanol (4ml) and acetonitrile (12ml). Then, methanolic solution of Et_3N (0.1mmol) was added to the solution, and the reaction mixture was stirred for 5min, after which $DyCl_3\cdot 6H_2O$ (0.2mmol) was added and the yellow solution was continually stirred for 30min.The resultant yellow solution was left unperturbed to

allow the slow evaporation of the solvent. Orange yellow single crystals, suitable for X-ray diffraction analysis, were formed after 10 days. Yield: 75.7mg (65%, based on the metal salt).Elemental analysis (%) calcd for $C_{13}H_{20}Cl_2DyN_3O_8$: C, 26.93, H, 3.48, N, 7.25; found C, 27.27, H, 3.61, N, 7.40. IR (KBr, cm^{-1}): 3283(br), 1634(s), 1603(s), 1545(s), 1487(m), 1472(m), 1435(m), 1391(m), 1334(w), 1314(m), 1250(w), 1197(m), 1152(m), 1036(w), 897(m), 838(w), 777(m), 757(w), 666(m), 599(w), 581(m), 523(w), 411(w).

X-ray crystallography and physical measurement

Intensity data for crystal of **1** was collected on a Bruker Smart Apex Ⅱ CCD diffractometer with graphite-monochromated Mo Kα radiation(0.71073 Å) at 296K. The structures were solved by direct methods and refined with the full-matrix least-squares technique based on F^2 using the SHELXL program. All non-hydrogen atoms were refined anisotropically. Hydrogen atoms were placed at the calculation positions. The details of crystallographic data and selected bond parameters for compounds **1** are listed in Table S1 and Table S2, respectively.

Elemental analyses of carbon, hydrogen, and nitrogen were carried out with an ElementarVario EL analyzer. FTIR spectra were recorded in the range of 4000 to $400cm^{-1}$ on an AVATAR 360 Nicolet 380 FT/IR spectrometer using KBr pellets. Powder X-ray diffraction (XRD) analyses were performed on a Rigaku Dmax-2000 X-ray diffractometer with Cu Kα (λ=1.54059 Å) radiation. Variable-temperature magnetic susceptibility measurements of **1** were performed on an SQUID-VSM and PPMS magnetometer.

Computational details

For CASSCF calculations, the basis sets for all atoms are atomic natural orbitals from the MOLCAS ANO-RCC library: ANO-RCC-VTZP for Dy^{3+} ion; VTZ for close O and N; VDZ for distant atoms. The calculations employed the second order Douglas-Kroll-Hess Hamiltonian, where scalar relativistic contractions were taken into account in the basis set and the spin-orbit coupling was handled separately in the restricted active space state interaction (RASSI-SO) procedure. The active electrons

in 7 active spaces include all *f* electrons (CAS(9 in 7)) in the CASSCF calculation. To exclude all the doubts we calculated all the roots in the active space. We have mixed the maximum number of spin-free state which was possible with our hardware (all from 21 sextets; 128 from 224 quadruplets; 130 from 490 doublets).

Table S1 Crystallographic Data and Structure Refinement for complex **1**

Formula	$C_{13}H_{20}Cl_2DyN_3O_8$	γ(°)	90
Mr	579.72	V (Å^3)	3932.4(3)
Cryst size (mm)	0.30*0.14*0.04	Z	8
Crystal system	Orthorhombic	μ (mm^{-1})	4.117
Space group	*P*bca	*F*(000)	2264
T(K)	300	GOF	1.068
a(Å)	14.9729(6)	Data collected	22585
b(Å)	14.7878(6)	Unique	4563
c(Å)	17.7603(7)	R_{int}	0.0247
a(°)	90	*R*1,*wR*2[*I* >2σ(*I*)]	0.0207, 0.0473
β(°)	90	R1, wR2 [all data]	0.0269, 0.0497

Table S2 Selected Bond Distances (Å) in complex **1**

Dy1-O1	2.463 (2)	Dy1-O2	2.377(2)	Dy1-O3	2.184(2)
Dy1-O4	2.359(2)	Dy1-O5	2.401(2)	Dy1-O6	2.426(2)
Dy1-O7	2.357(2)	Dy1-N3	2.556(2)		

Table S3 Hydrogen Bonds in **1**.

D-H	d(D-H) (Å)	<DHA(°)	d(D…A) (Å)	A
N2-H2A	0.860	130.34	2.618	O1
O4-H4A	0.935	163.61	3.120	Cl1[-x+1,-y+1,-z+1]
O5-H5A	0.936	169.37	3.104	Cl1[x,-y+1/2,z-1/2]
O6-H6A	0.927	161.75	3.139	Cl1[x,-y+1/2,z-1/2]
O7-H7A	0.935	166.24	3.067	Cl1[x+1/2,-y+1/2,-z+1]
O6-H6B	0.920	165.95	3.069	Cl2[-x+3/2,y-1/2,z]
O7-H7B	0.924	165.15	3.070	Cl2[-x+3/2,y-1/2,z]
O5-H5B	0.933	169.75	2.781	O8
O4-H4B	0.935	178.79	3.119	Cl2[x-1/2,y,-z+1/2]
O8-H8A	0.937	132.06	3.266	Cl2[x-1/2,y,-z+1/2]

O8-H8A	0.937	133.16	3.525	Cl2[-x+3/2,-y+1,z+1/2]

Table S4. Energy (cm^{-1}) of the lowest calculated Kramers doublets (KDs) and the ground *g* tensor of the Dy^{3+} fragment.

Energy of eight lowest KDs	*g* tensor of the ground KD
0.000	$g_x = 0.0039$ $g_y = 0.0099$ $g_z=19.6859$
187.486	
213.684	
315.532	
391.831	
481.099	
535.748	
625.723	

Table S5 Relaxation fitting parameters from Least-Squares Fitting of $\chi(f)$ data under zero dc field of **1**.

T (K)	χ_T	χ_S	α	τ (s)
2	4.55	0.08	0.23	9.55E-4
4	2.34	0.05	0.24	1.02E-3
6	1.54	0.04	0.24	8.71E-4
8	1.15	0.035	0.23	7.32E-4
10	0.91	0.033	0.22	6.08E-4
12	0.74	0.032	0.18	4.57E-4
12.5	0.71	0.032	0.16	4.19E-4
13	0.67	0.032	0.14	3.77E-4
13.5	0.64	0.032	0.13	3.36E-4
14	0.61	0.032	0.11	2.99E-4
14.5	0.59	0.031	0.097	2.65E-4
15	0.57	0.031	0.084	2.31E-4
15.5	0.54	0.030	0.071	1.99E-4
16	0.52	0.030	0.060	1.70E-4
16.5	0.51	0.027	0.052	1.43E-4
17	0.50	0.026	0.056	1.17E-4
17.5	0.48	0.026	0.045	9.53E-5
18	0.47	0.021	0.056	7.56E-5
18.5	0.46	0.021	0.052	5.93E-5
19	0.44	0.015	0.064	4.57E-5
19.5	0.43	0.003	0.086	3.41E-5
20	0.42	0.012	0.068	2.65E-5
20.5	0.41	0.008	0.085	1.99E-5
21	0.40	0.005	0.096	1.49E-5
21.5	0.39	0.005	0.11	1.13E-5
22	0.38	0.003	0.136	8.35E-6

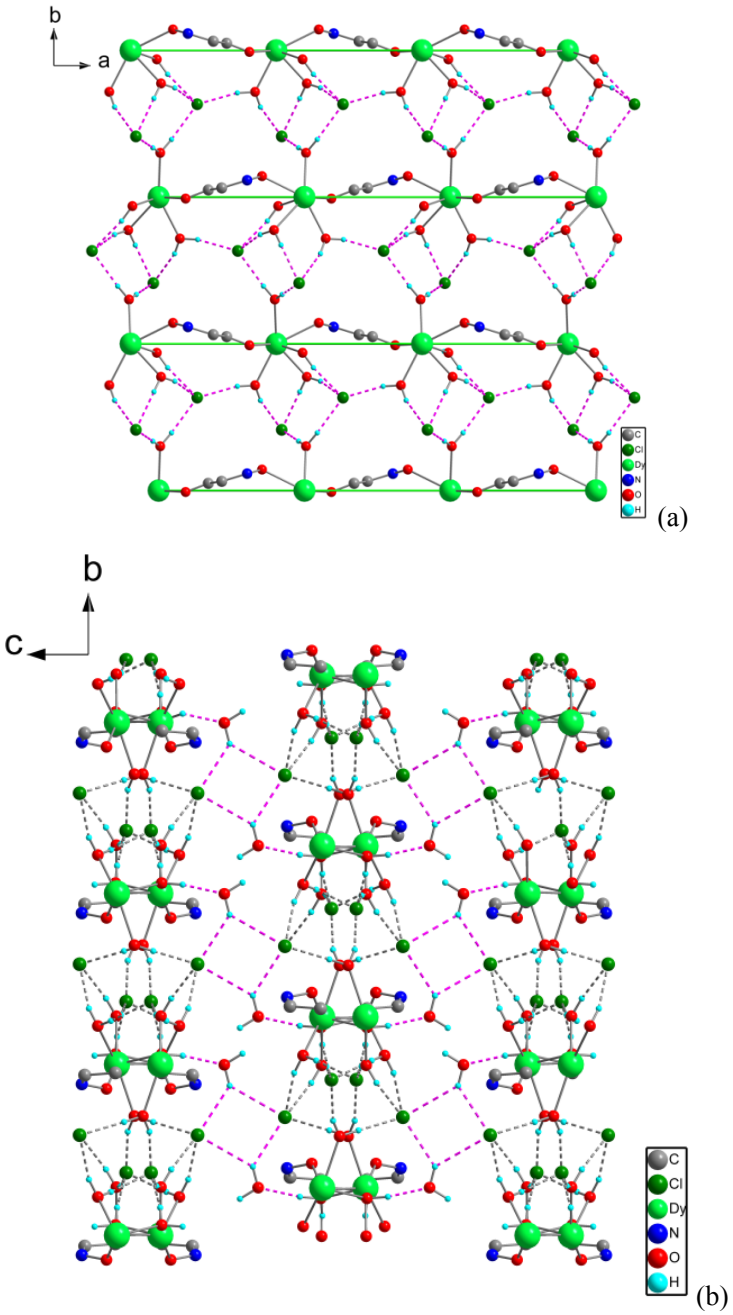

Fig. S1 2D sheet (a) and 3D supramolecular structure (b) of compound **1** constructed by hydrogen bonds.

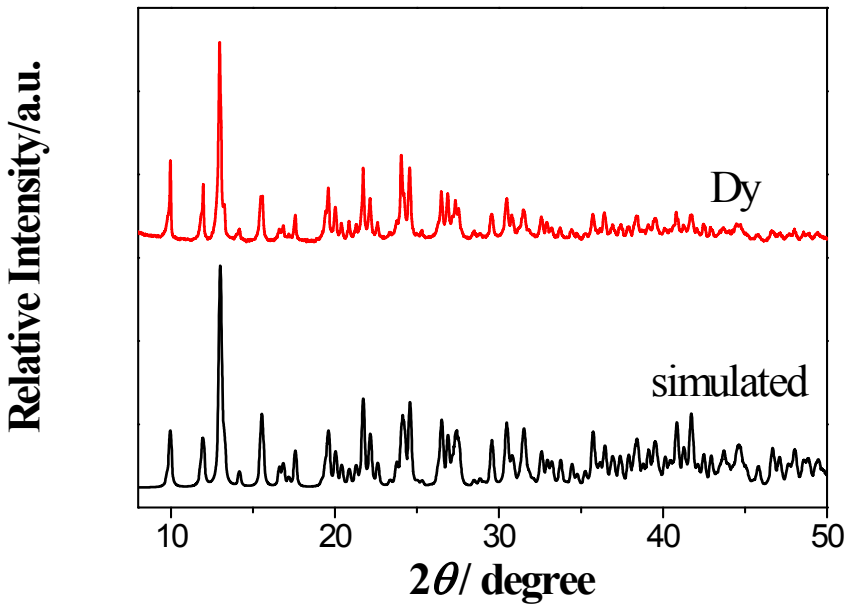

Fig. S2 Powder X-ray diffraction profiles of **1** together with a simulation from the single crystal data.

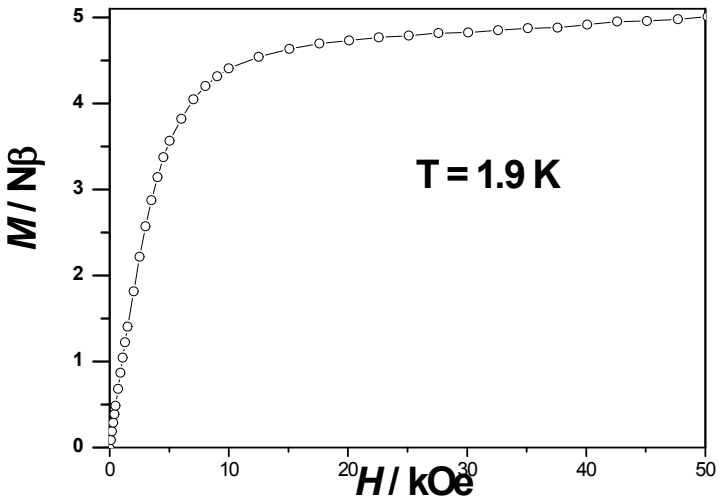

Fig. S3 Field dependence of the magnetization of **1** at 1.9K.

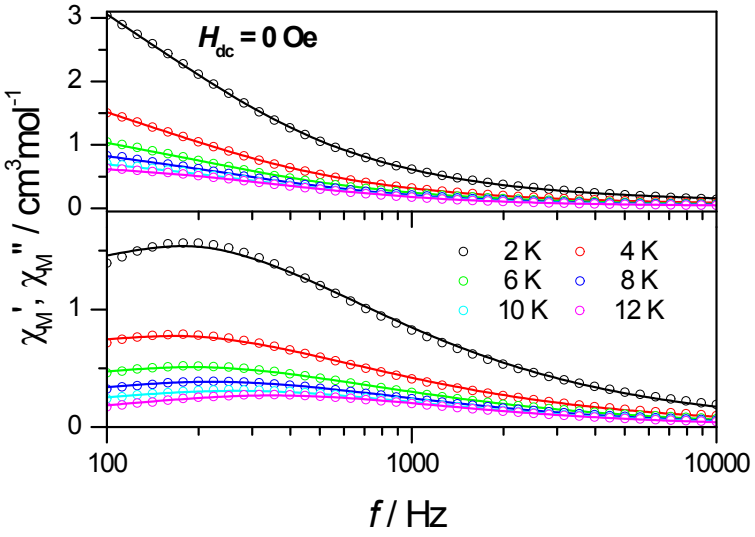

(a)

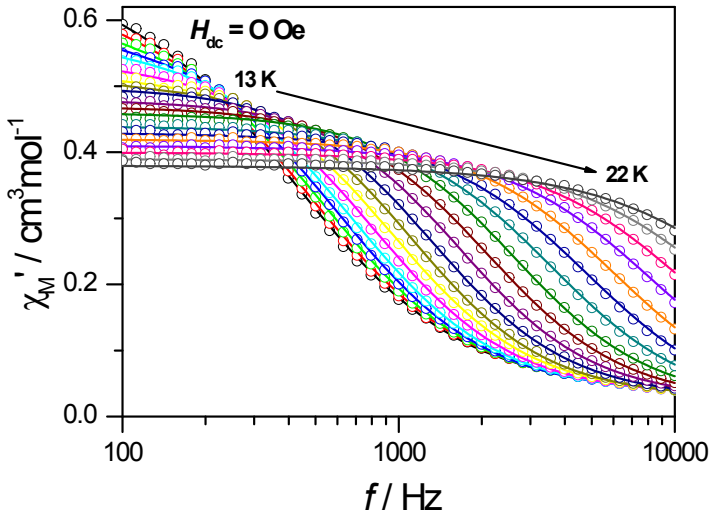

(b)

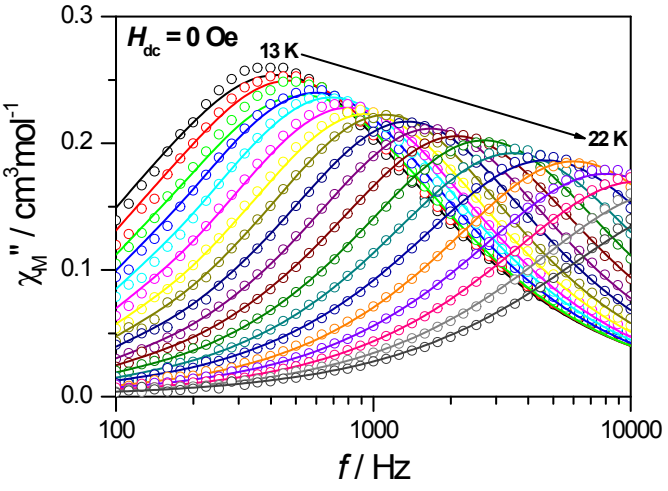

(c)

Fig. S4 *Ac-f* curves measured under zero *dc* fields for **1** at selected temperatures. Solid lines were fitted using a generalized Debye relaxation model, simultaneously to χ'(*f*) and χ" (*f*) curves.

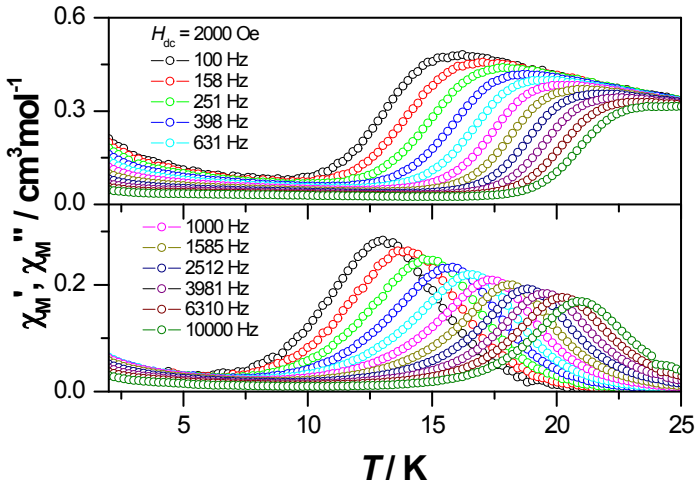

Fig. S5 The temperature dependence of ac susceptibility under 2000 Oe field for **1.**

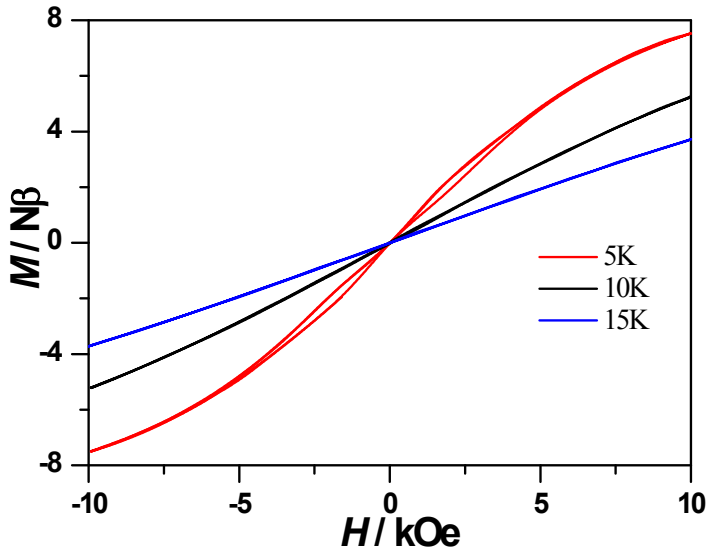

(a)

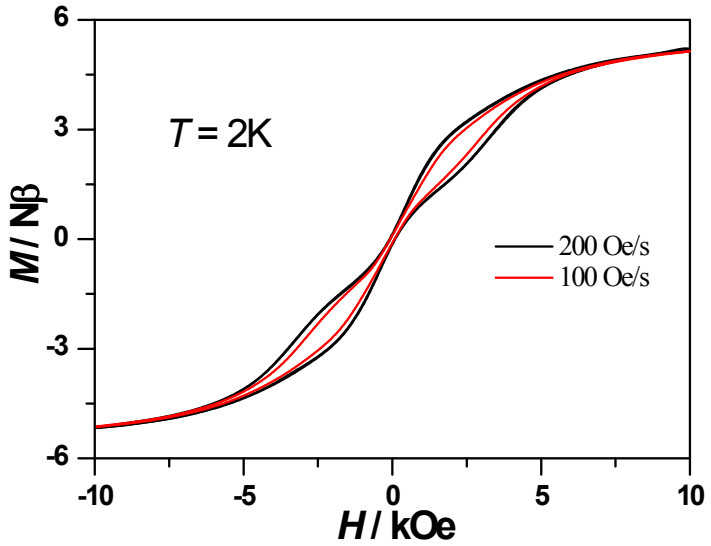

(b)

Fig. S6 Hysteresis loop for **1** measured at different temperatures with sweep rates of 200 Oe/s (a) and different sweeping rates at 2K (b).